Numerical Approach on the Mechanism of Precipitation-Topography Relationship in Mountainous Complex Terrain

Yoshiharu, S. [1], S. Miyata [2], E. Nakakita [3] and M. Hasebe [4]

[1] Faculty of Engineering, Utsunomiya University, Japan
[2] CTI Engineering Co., Ltd., Japan
[3] Disaster Prevention Research Institute, Kyoto University, Japan
[4] Faculty of Engineering, Utsunomiya University, Japan
Email: ysuzuki@cc.utsunomiya-u.ac.jp

Keywords: *precipitation-topography relationship, mesoscale meteorological model, orographic precipitation, mountainous terrain, topographic elevation*

EXTENDED ABSTRACT

The current study attempted to clarify how precipitation amount is connected with topographic elevation from a quantitative perspective and to elucidate the mechanisms of orographic effects on precipitation through physically-based numerical simulations of the atmosphere on a virtually-created isolated mountain. Fluctuation characteristics of the precipitation-topography relationship (P-T relationship) were also explored based on numbers of such experimental simulations with various cases of the height of the mountaintop, the base width of the mountain, the velocity of the environmental (synoptic-scale) wind, and the degree of the atmospheric instability shown by the CAPE value. It was found that a distinctive P-T relationship designated as ``the Gaussian-functional Relationship over an Isolated Mountain (GRIM)" can be created over an isolated mountain especially on its windward-side slope. The stratified sampling averages of the P-T relationship on the windward-side slope are approximated with high accuracy by the quadratic function, and those on the leeward-side slope also form a curved line roughly following the regression curve, although they include some undulations. The GRIM relationship is basically determined by three parameters representing the rate of change in precipitation following the change of topographic elevation, the peak position of precipitation, and the peak precipitation respectively.

The P-T relationship over an isolated mountain can be determined by the three primary factors, (1) the advection velocity of a cumulus cloud, (2) the growth rate of a cumulus cloud, and (3) the rate of change in topographic elevation. As a result of some investigations base on simulation results, it was found that the 1st factor is almost constant, the 2nd factor shows a Gaussian-functional variation, and the 3rd factor is always fixed in the process through which cumulus clouds are generated and developed one after another. Therefore, the formation of the GRIM, i.e., the Gaussian-functional relationship over an isolated mountain between accumulated precipitation and topographic elevation, is essentially derived from the 2nd factor, i.e., the Gaussian-functional variation in the growth rate of a cumulus cloud. Although the detailed processes of such variation in the growth rate of a cumulus cloud, or the reason why the development of a cumulus cloud show such variation, still remain unexplained, the fundamental mechanisms of the formation of the GRIM have been clarified.

Simulation results under various conditions of topography and the atmosphere showed that the GRIM relationship can be clearly formed on the windward side of an isolated mountain with no major bias of stratified sampling averages against the GRIM, meaning that the formation of the GRIM relationship is universal on the windward side. The peak position and curvature of the GRIM are sensitively affected by topographic and atmospheric conditions and the GRIM relationship can be in various forms of quadratic functions. The peak position of precipitation tends shift toward the leeward side as the velocity of the environmental wind increases, and more precipitation tends to be generated on the windward side when the velocity of the wind is lower. The place where initial precipitation is generated, in particular, is greatly affected by the velocity of the wind, being located further toward the windward side when the velocity of the wind is lower. Fluctuation characteristics of the GRIM parameters will be explored from a quantitative perspective in the next phase, which will contribute toward developing a disaggregation model of precipitation based on the detailed characteristics of the P-T relationship.

1. INTRODUCTION

Some investigations in the past simulated the precipitation-topography relationship (the P-T relationship), using a numerical meteorological model, to understand its physical mechanism (e.g., Colton 1976, Alpert 1986, Barros and Lettenmaier 1994, Oishi *et al.* 1997). Through simulations with actual conditions of the height of a mountain, the slope of a mountain or the velocity and direction of the wind, part of the principal factors which determine the amount and the distribution of precipitation were clarified. As one of the mechanisms of orographic precipitation, the Seeder-Feeder effect has also been clarified through some empirical and numerical studies (e.g., Smith 1979), which is orographic enhancement of precipitation over hills through the washout of cloud droplets in lower atmosphere. However, many of the past numerical studies focused on a particular physics process of precipitation or a particular case of atmospheric phenomena, and thus, there were few investigations aimed at elucidating universal or statistical characteristics of the P-T relationship.

On the other hand, some studies conducted experimental simulations using a numerical model with virtually-created conditions of topography and the atmosphere to see general features of precipitation distribution. Through two-dimensional numerical simulations of the atmosphere which introduced virtually-created topography, Hibino (1995) showed that the position with precipitation peak tends to vary greatly according to the strength of the synoptic-scale wind, and that the simulations with a higher mountain display a stronger tendency to shift the precipitation area toward the windward side of the mountain. Oishi (1997) also conducted two-dimensional simulations using a cloud physics model with a bell-shaped isolated mountain and clarified the influence of the strength and vertical shear of the wind, and the horizontal scale of the mountain, etc., on the development process of cumulus clouds. Nevertheless, such conventional studies have not found any effective techniques for the quantitative assessment of the P-T relationship, and have not led to a comprehensive and deeper understanding of the relationship including its universality and singularity.

In the current study, in order to clarify the detailed mechanisms of the P-T relationship in mountainous regions, three-dimensional numerical experiments are conducted using the mesoscale meteorological model MM5. Through physically-based numerical simulations of the atmosphere on a virtually-created isolated mountain, it is attempted to clarify how precipitation amount is connected with topographic elevation from a quantitative perspective and to determine the mechanisms of orographic effects on precipitation. As the first step for the formulation of the P-T relationship, it is discussed what effect and how much effect topographic and atmospheric conditions have on the relationship.

2. DESCRIPTION OF EXPERIMENTAL NUMERICAL SIMULATIONS

2.1. Model Configurations

MM5 contains a multiple-nest capability and a four-dimensional data assimilation capability. Such model options are, however, not employed for the experimental simulations of the atmosphere in the current study. The model options for physical process schemes except the explicit moisture scheme, i.e., the land surface scheme and the planetary boundary layer scheme, etc., are also not employed since the main objective in the current study is the effects of topography on daily or monthly precipitation, or the Mesoβ-scale P-T relationship. Mixed-Phase ice scheme (Grell *et al.* 1994, Reisner *et al.* 1998) was employed for the explicit moisture scheme. The model also is set up to exclude the effects of the map factor and Coriolis force from the simulations.

The model grid size is 3 (km), and the simulation area covers 120 by 120 grids field. Simulations with the simulation period of 6 hours and the computing time step of 9 seconds were conducted under constant boundary conditions. The study area was, however, limited to the central area with 60 by 60 grids (180 by 180 km) to avoid the influence of the boundary conditions being constant as much as possible. Investigations of the P-T relationship described in the following sections are mainly based on 6-hours-accumulated precipitation from simulation results.

2.2. Atmospheric Conditions

As for initial conditions of the atmosphere, on the assumption that the atmosphere is in a state where convective precipitation readily triggered by mountains, the conditional unstable atmosphere was created in which the lifting condensation level (LCL) roughly corresponding to the cloud base height is 1400 m (approximately 850 hPa) and the level of neutral buoyancy (LNB) roughly corresponding to the cloud top height is 7400 m (approximately 390 hPa). The vertical profile of atmospheric conditions created in the current study is shown in Figure 1. The figure shows the profile of potential temperature, equivalent potential temperature and relative humidity. Horizontally uniform conditions of the atmosphere shown in this

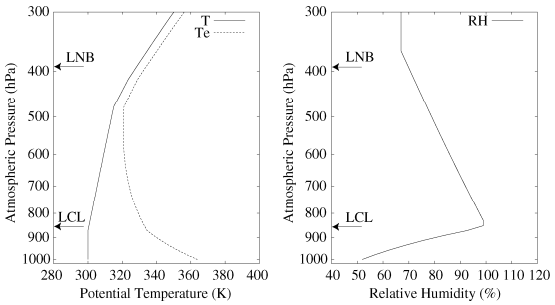

Figure 1. Vertical profile of the atmosphere used for initial conditions of MM5, including potential temperature (left, solid line), equivalent potential temperature (left, broken line) and relative humidity (right). LCL and LNB denote the lifting condensation level and the level of neutral buoyancy.

figure were introduced into the model as its initial and boundary conditions. By reference to atmospheric conditions employed by Oishi (1997), the profile of relative humidity was created with the mixing ratio of water vapor being constant from the ground to a height of 1.4 (km) and decreasing with a height above the height of 1.4 (km), which roughly represents actual conditions of the atmosphere including a convective cloud.

To see the degree of the atmospheric instability, the value of the Convective Available Potential Energy (CAPE) is calculated based on the vertical profile of atmospheric conditions. The value of the CAPE represents the magnitude of buoyancy which lifts the air parcel into the upper air, and a greater value of the CAPE means a higher degree of the atmospheric instability. The value of the CAPE calculated for the atmospheric profile in Figure 1 is 834 (m^2/s^2). Some atmospheric profiles with different values of the relative humidity near the ground level are employed to incorporate the variations of the atmospheric instability, shown by the CAPE value, into the experimental simulations.

Initial and boundary conditions of the environmental (synoptic-scale) wind were created, in which the whole simulation area has uniform values of the direction and velocity of the wind at the beginning of the simulations, and the boundary values of them are kept constant during the simulations. The velocity of the environmental wind is considered to have so great effect on the P-T relationship that various atmospheric conditions with different values of the wind velocity were introduced into the model.

2.3. Topographic Conditions

As for topographic conditions including an isolated mountain, since the current study focuses on

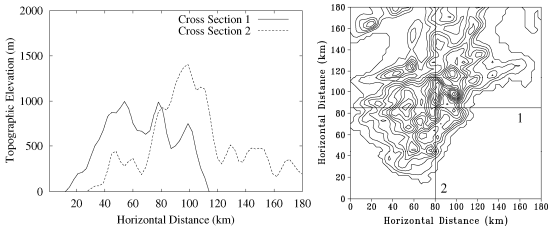

Figure 2. Example of the shape of mountains in the southern Kinki region of Japan, showing vertical cross sections of mountains (left) and the contour map of elevation with lines corresponding to the sections (right).

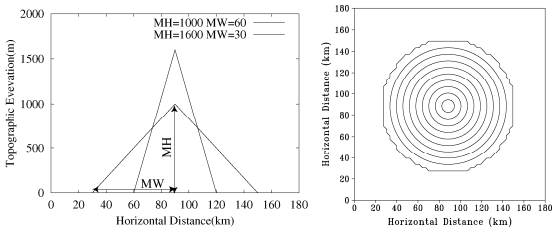

Figure 3. Example of the conical-shape mountains used for experimental simulations, showing two cases of its vertical cross section passing on the mountaintop (left) and the contours of elevation on the mountain with HM of 1000 (m) and WM of 60 (km) (right).

the P-T relationship over mountains with the same spatial scale as those in Japan, the shape and spatial scale of some actual mountains in Japan were briefly examined. An example of the shape of mountains is shown in Figure 2. The figure shows a vertical cross section of mountains in the southern Kinki region of Japan based on elevation data whose resolution scale is 3 (km). The shape of the mountains seems to be generally represented by a superposition of mountains with a triangular-shaped cross section, which is a common feature to other mountains in Japan. Therefore, the current study introduces a conical-shaped isolated mountain whose shape in a vertical cross section is triangular, as shown in Figure 3, into the topographic condition of the model. The shape of the mountain is, thus, determined by two parameters which represent the height of the mountaintop and the horizontal scale (i.e., the base width) of the mountain.

3. PRECIPITATION-TOPOGRAPHY RELATIONSHIP OVER AN ISOLATED MOUNTAIN

In the current study, experimental simulations with a virtually-created isolated mountain are conducted with various cases of the height of the mountaintop (denoted by HM), the base width of the mountain (denoted by WM), the velocity of the environmental (synoptic-scale) wind (denoted by VW),

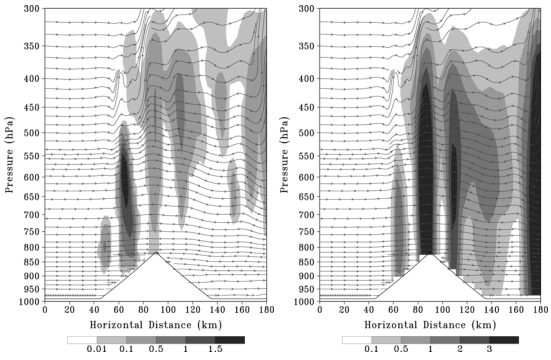

(a) Cumulus Clouds (b) Precipitation

Figure 4. Results of the simulation conducted with HM of 1600 (m), WM of 45 (km), VW of 10 (m/s) and CP of 834 (m^2/s^2), showing an instantaneous image of cumulus clouds (left) and precipitation (right) at 180 minutes after the beginning of the simulation. The former is represented by the sum of the two mixing ratios of cloud water and ice water, and the latter by those of rain water and snow.

and the degree of the atmospheric instability shown by the CAPE value (denoted by CP). Since the state of the atmosphere simulated tends to be into a stationary state in around 6 hours after the beginning of the simulations due to constant boundary conditions, investigations in the following sections are mainly based on 6-hours-accumulated precipitation. It is difficult to discuss, from a quantitative perspective, how the temporal scale of 6 hours or the amount of precipitation in the period in experimental simulations corresponds to those in actual precipitation events, nevertheless the characteristics of precipitation in 6 hours from the simulation results can be considered to be representative of those in actual daily precipitation or each precipitation event.

An example of the simulation results is shown in Figure 4, which is the case with HM of 1600 (m), WM of 45 (km), VW of 10 (m/s) and CP of 834 (m^2/s^2). The left figure shows an instantaneous image of cumulus clouds and the right figure shows that of precipitation in the vertical cross section passing over the mountaintop at the point in time of 180 minutes after the start of computing. The horizontal axis represents a horizontal distance and vertical axis represents the vertical distribution of the atmospheric pressure. The wind is from the constant direction of the left-hand side of the figures at all times during the simulation. The cumulus clouds are generated and developed one after another on the windward side of the mountain and transported to the leeward side of the mountain, while the precipitation is generated from the clouds with its intensity changing. The clouds in the figures are represented by the summation of the

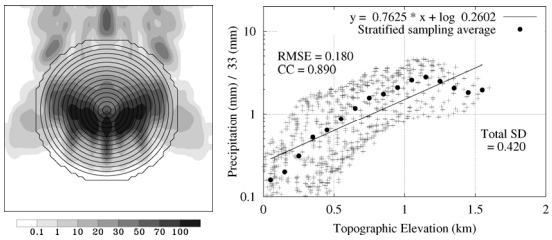

(a) Velocity of the Wind (VW) of 8 m/s (Case-1)

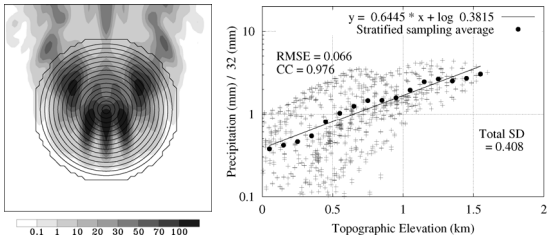

(b) Velocity of the Wind (VW) of 10 m/s (Case-2)

Figure 5. Results of the simulation conducted with each velocity of the wind (VW) and with HM of 1600 (m), WM of 60 (km) and CP of 834 (m^2/s^2), showing the distribution of 6-hours-accumulated precipitation (mm) (left) and its precipitation-elevation correlation including the ECAT (right). In the left figures, the horizontal wind runs from the bottom to the top, and the contours denote topographic elevation.

mixing ratio of cloud water and ice water, and the precipitation is represented by that of rain water and snow. These simulation results demonstrate that the configurations of the model used in the current study are proper enough to reproduce typical characteristics of the actual atmospheric phenomena with precipitation.

Figure 5 shows examples of the distribution of 6-hours-accumulated precipitation in the left figures, and its precipitation-elevation correlation in the right figures. The figures (a) is the case (denoted by Case-1) with HM of 1600 (m), WM of 60 (km), VW of 8 (m/s) and CP of 834 (m^2/s^2), and the figures (b) is the case (denoted by Case-2) with VW of 10 (m/s), in which other indexes are the same with (a). The left figures, in which the horizontal wind runs from the bottom to the top, show the difference of how the precipitation is distributed on the mountain between the two cases of VW. The precipitation tends to be concentrating on the windward-side slope close to the mountaintop. In the right figures, the stratified sampling averages in Case-1 represented with the black circles form a curved line similar to a parabolic curve, and, to the contrary, there seems a linear relationship among the stratified sampling averages in Case-2.

The precipitation-elevation correlation in Case-1 and Case-2 where the area on the mountain is di-

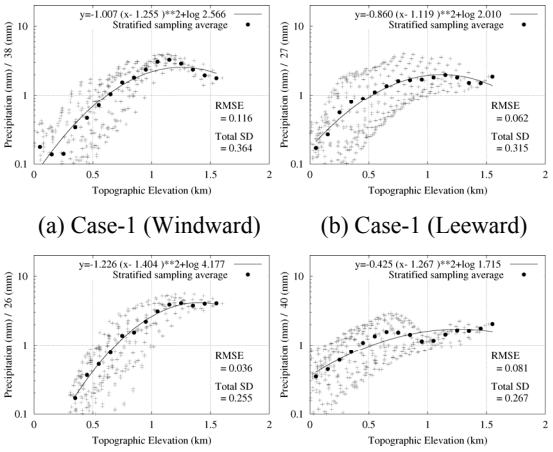

(a) Case-1 (Windward) (b) Case-1 (Leeward)

(c) Case-2 (Windward) (d) Case-2 (Leeward)

Figure 6. Precipitation-elevation correlation in Case-1 and Case-2 with dividing the area into the windward (left) and leeward (right) of the mountain, including a regression curve approximated with a quadratic function for the stratified sampling averages.

vided into two parts of the windward and leeward side is shown in Figure 6, including a regression curve approximated with a quadratic function for the stratified sampling averages. In the approximation, some classes of elevation stratification were excluded when the stratified sampling average in each class is less than 10 percent of the areal average precipitation (AAP), which is represented by the value of 0.1 on the vertical axis. The figures show that the stratified sampling averages on the windward-side slope, especially in Case-2, are approximated with high accuracy by the quadratic function, and that those on the leeward-side slope also form a curved line roughly following the regression curve, although they include some undulations. This relationship seems to be one of the distinctive characteristics of the P-T relationship over an isolated mountain, especially on the windward-side slope, although it has not ever been reported in the previous studies.

4. FUNDAMENTAL MECHANISMS OF THE FORMATION OF THE GRIM

Some investigations are, then, conducted into the mechanisms which produce the formation of GRIM. The process through which cumulus clouds are generated and developed one after another is analyzed based on the simulation result of Case-2 shown in Figure 6. The temporal variation of precipitation intensity during the simulation of Case-2 is shown in Figure 7. The figure shows the value of one-minute-average intensity of precipitation at ground level on the line passing through the mountaintop in the environmental wind direction. The horizontal axis is the computing time after the beginning of the simulation, and the vertical axis is the horizontal distance from a windward-side point on the line passing through the mountaintop, on which the top is located at the point of 90 (km). Each of the oval-form shading areas shown in the figure represents a cumulus cloud, which is generated and developed one after another during the simulation. Although there are slight differences among the individual cumulus clouds in the position where they are generated or the peak amount of precipitation, they have basically common features in the process through which they are advected or the amount of precipitation varies.

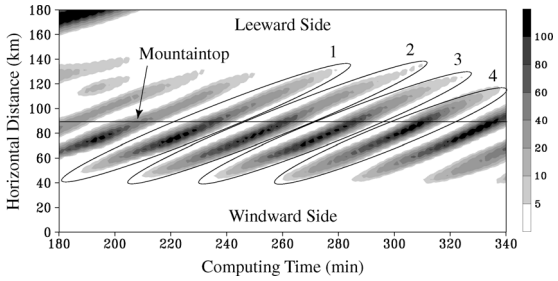

Figure 7. Temporal variation of precipitation intensity during the simulation of Case-2, shown with the value of one-minute-average precipitation (mm) at ground level on the line passing through the mountaintop in the environmental wind direction.

Here, when our attention is turned to Figure 4 showing the motion and variation of cumulus clouds generated by the mountain, the following three factors seem to be essential as a primary factor which determines the P-T relationship over an isolated mountain.

(1) Advection velocity of a cumulus cloud
(2) Growth rate of a cumulus cloud
(3) Rate of change in topographic elevation

The last one represents how the topographic elevation under a cumulus cloud changes during its advection. The current study focuses on the cumulus clouds circled in Figure 7 (denoted by Cloud-1 to Cloud-4), and examines the above three factors, assuming that the position of a cumulus cloud is represented by the peak position of precipitation produced from the cloud, and assuming that the growth of a cumulus cloud can be assessed by the intensity of the peak precipitation.

Firstly, to see the variation of ``the advection velocity of a cumulus cloud'', it was investigated how long it is for the peak position of precipitation in Cloud-1 to Cloud-4 to move across a model grid whose size is 3 (km). The result is in Figure 8, showing the relation between the number of a

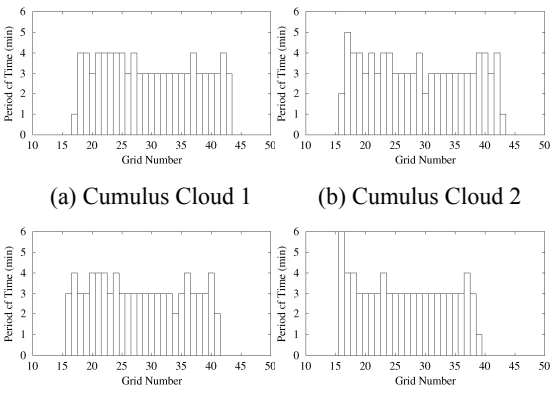

(a) Cumulus Cloud 1 (b) Cumulus Cloud 2

(c) Cumulus Cloud 3 (d) Cumulus Cloud 4

Figure 8. Advection velocity of cumulus clouds, represented by the period of time required for the peak position of precipitation in each cumulus cloud to move across a model grid whose size is 3 (km). The grid number on the horizontal axis denotes the horizontal moving distance of the peak position. The number assigned to each cumulus cloud corresponds to that shown in Figure 7.

model grid and a period of time required for the movement. It was assumed in this investigation that a cumulus cloud is generated when the peak amount of precipitation in the cloud exceeds 0.1 (mm). In the figures, the period of time for moving across a model grid shows a small variation in every case, meaning that the advection velocity of a cumulus cloud is almost constant after its generation. Therefore, a cumulus cloud generated by topography tends to be advected at a nearly constant speed with little influence of topography on its advection speed, when there are little fluctuations in the environmental wind. The advection speed, however, seems to vary according to the form of the mountain, on which the cumulus cloud was generated, and depend on the velocity of the environmental wind.

Secondly, an investigation was conducted into how the intensity of peak precipitation in Cloud-1 to Cloud-4 tends to vary during its advection in order to assess ``the growth rate of a cumulus cloud''. Figure 9 shows the relation on a semi-logarithmic plot between a period of time and the intensity of peak precipitation after the generation of each cumulus cloud. In the figures, the intensity of peak precipitation in every cumulus clouds shows a tendency to vary, with the passage of time, roughly following a quadratic function. This indicates, where it is taken into account that the vertical axis is on a logarithmic scale, that the growth rate of a cumulus cloud tends to show a Gaussian-functional variation. There is a subtle difference in the growth rate among the four cases, and also between in the growth and decline period of each cumulus cloud. However, the whole variation of

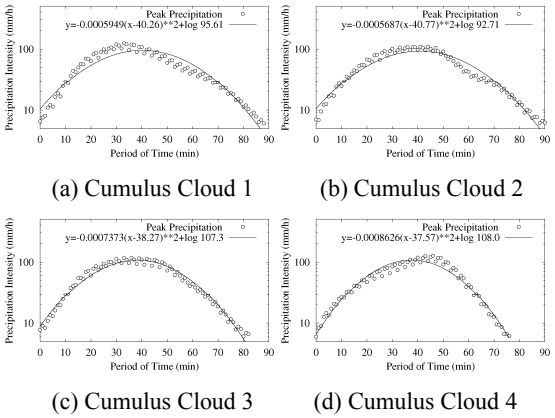

(a) Cumulus Cloud 1 (b) Cumulus Cloud 2

(c) Cumulus Cloud 3 (d) Cumulus Cloud 4

Figure 9. Temporal variation of the intensity of peak precipitation in each cumulus cloud during its advection, shown on a semi-logarithmic plot. The horizontal axis represents the period of time after the generation of the cloud. The number assigned to each cloud corresponds to that in Figure 7.

each cloud during its lifetime of around 80 to 90 minutes is approximated with sufficient accuracy by the quadratic function.

Finally, ``the rate of change in topographic elevation'' can be considered to be always fixed because a conical-shaped isolated mountain, whose shape in a vertical cross section is triangular, is employed in the simulations. An examination was also conducted into the case with a variable rate of change in topographic elevation to clarify the influence of a mountain shape. The result showed that it has little influence on the functional form of the P-T relationship, although there was a certain amount of gaps in such cases between the form of the P-T relationship and a quadratic-functional regression curve. Based on this result as well as the fact that the shape of actual mountains can be represented by a superposition of mountains with a triangular-shaped cross section, there is no essential need to take into consideration the case with a variable rate of change in topographic elevation.

The above results can be briefly summarized as follows; the 1st factor ``the advection velocity of a cumulus cloud'' is almost constant, the 2nd factor ``the growth rate of a cumulus cloud'' shows a Gaussian-functional variation, and the 3rd factor ``the rate of change in topographic elevation'' is always fixed. It follows from these that the formation of the GRIM, i.e., the Gaussian-functional relationship over an isolated mountain between accumulated precipitation and topographic elevation, is essentially derived from the 2nd one, i.e., the Gaussian-functional variation in the growth rate of a cumulus cloud. Although the detailed processes of such variation in the growth rate of a cumulus cloud, or the reason why the development

of a cumulus cloud show such variation, still remain unexplained, the fundamental mechanisms of the formation of the GRIM have been clarified in the current study.

5. CONCLUSION

The current study attempted to clarify how precipitation amount is connected with topographic elevation from a quantitative perspective and to elucidate the mechanisms of orographic effects on precipitation through physically-based numerical simulations of the atmosphere on a virtually-created isolated mountain. It was found that a distinctive P-T relationship designated as ``the Gaussian-functional Relationship over an Isolated Mountain (GRIM)" can be created over an isolated mountain especially on its windward-side slope. Fundamental mechanisms of the GRIM formation were clarified by analyzing the development process of convective cells.

Through additional simulations under various conditions of topography and the atmosphere, the GRIM relationship was found to be clearly formed on the windward side of an isolated mountain with no major bias of stratified sampling averages against the GRIM (e.g., Figure 10), meaning that the formation of the GRIM relationship is universal on the windward side. The peak position and curvature of the GRIM are sensitively affected by topographic and atmospheric conditions and the GRIM relationship can be in various forms of quadratic functions. The peak position of precipitation tends shift toward the leeward side as the velocity of the environmental wind increases, and more precipitation tends to be generated on the windward side when the velocity of the wind is lower. The place where initial precipitation is generated, in particular, is greatly affected by the velocity of the wind, being located further toward the windward side when the velocity of the wind is lower. Fluctuation characteristics of the GRIM parameters will be explored from a quantitative perspective in the next phase, which will contribute toward developing a disaggregation model of precipitation based on the detailed characteristics of the P-T relationship.

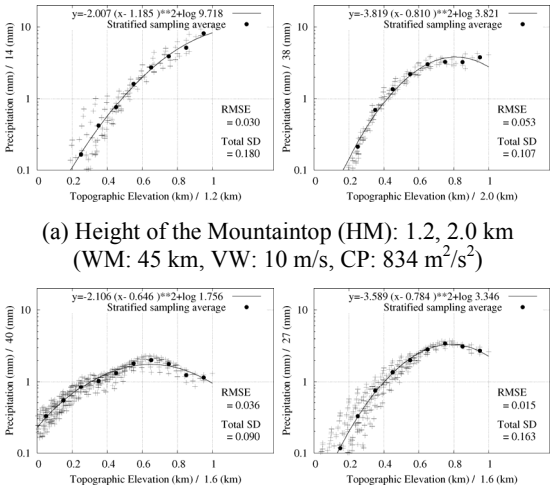

(a) Height of the Mountaintop (HM): 1.2, 2.0 km (WM: 45 km, VW: 10 m/s, CP: 834 m^2/s^2)

(b) Velocity of the Wind (VW): 6, 10 m/s (HM: 1.6 km, WM: 60 km, CP: 834 m^2/s^2)

Figure 10. Simulation results of the precipitation-elevation correlation on the windward side, including the GRIM relationship, under various conditions of topography and the atmosphere.

6. REFERENCES

Alpert, P. (1986), Mesoscale indexing of the distribution of orographic precipitation over high mountains, *J. Clim. Appl. Meteor.*, 25, 532-545.

Colton, D. E. (1976), Numerical simulation of the orographically induced precipitation distribution for use in hydrologic analysis, *J. Appl. Meteor.*, 15(12), 1241-1251.

Barros, A. P., and D. P. Lettenmaier (1994), Dynamic modeling of orographically induced precipitation, *Rev. Geophys.*, 32(3), 265-284.

Grell, G. A., J. Dudhia, and D. R. Stauffer (1994), A description of the fifth-generation Penn State/NCAR mesoscale model (MM5), TNCAR Technical Note, NCAR/TN-398+STR.

Hibino, T. (1995), Study on the characteristics of rainfall in mountainous basins (in Japanese), Ph.D. thesis, Chuo Univ.

Oishi, S., Y. Kitani, E. Nakakita, and S. Ikebuchi (1997), Numerical approach on effect of topography to severe rainfall using non-parameterized cloud microphysics model (in Japanese with an English abstract), *Ann. J. Hydraul. Eng.*, 41, 117-122.

Reisner, J., R. J. Rasmussen, and R. T. Bruintjes (1998), Explicit forecasting of supercooled liquid water in winter storms using the MM5 mesoscale model, *Quart. J. Roy. Meteor. Soc.*, 124B, 1071-1107.

Smith, R. B. (1979), The influence of mountains on the atmosphere, *Adv. Geophys.*, 21, Ed. B. Saltzman, Academic Press, New York, 87-230.